

ST-MODULATOR: MODULATING SPACE-TIME ATTENTION FOR MULTI-GRAINED VIDEO EDITING

Anonymous authors

Paper under double-blind review



Figure 1: ST-Modulator enables multi-grained video editing across class, instance, and part levels.

ABSTRACT

Recent advancements in diffusion models have significantly improved video generation and editing capabilities. However, multi-grained video editing, which encompasses class-level, instance-level, and part-level modifications, remains a formidable challenge. The major difficulties in multi-grained editing include semantic misalignment of text-to-region control and feature coupling within the diffusion model. To address these difficulties, we present ST-Modulator, a zero-shot approach that modulates space-time (cross- and self-) attention mechanisms to achieve fine-grained control over video content. We enhance text-to-region control by amplifying each local prompt’s attention to its corresponding spatial-disentangled region while minimizing interactions with irrelevant areas in cross-attention. Additionally, we improve feature separation by increasing intra-region awareness and reducing inter-region interference in self-attention. Extensive experiments demonstrate our method achieves state-of-the-art performance in real-world scenarios. More details are available on the [project page](#).

1 INTRODUCTION

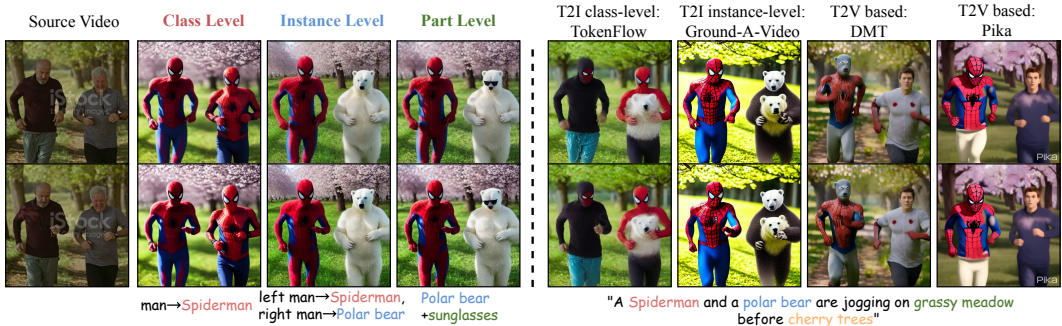


Figure 2: Definition of multi-grained video editing and comparison on instance editing

Recent advances in Text-to-Image (T2I) and Text-to-Video (T2V) diffusion models (Rombach et al., 2022; Chen et al., 2024; Wang et al., 2023a; Brooks et al., 2024) have enabled video manipulation through natural language prompts. In practical applications, enabling users to edit regions at various levels of granularity based on textual prompts offers greater flexibility. To investigate this, we introduce a new task called multi-grained video editing, which encompasses class-level, instance-level, and part-level editing, as shown in Fig. 2 left. Class-level editing refers to modifying objects within the same class. Instance-level editing means editing different instances into distinct objects. Part-level going further, requires adding new objects or modifying existing attributes at part-level.

While existing methods employ various visual consistency techniques, such as optical flow (Cong et al., 2023; Yang et al., 2023), control signals (Zhang et al., 2023b), or feature correspondence (Geyer et al., 2023). These methods remain instance-agnostic, often mixing features of different instances during editing (see Fig. 2 right). Ground-A-Video (Jeong & Ye, 2023), which inherits text-to-bounding box generation priors (Li et al., 2023), should be instance-level editing but still suffer from artifacts. Similarly, recent T2V-based methods like DMT (Yatim et al., 2024) and Pika (pik), although equipped with video generation priors, struggle with multi-grained edits. We find that the core issue is that diffusion models tend to treat different instances as the same class segments, leading to strong feature coupling across instances, as illustrated in Figure 3.

To address this problem, our primary insight is to 1) enable text-to-region control and 2) keep feature separation between regions. In the typical diffusion models, the cross-attention layer serves as a key component to update textual features control over each spatial region, while the self-attention layer generates globally coherent structures by connecting each frame token across time. Therefore, we propose Spatial-Temporal Layout-Guided Attention (ST-Layout Attn), which modulates both space-time cross- and self-attention in a unified manner to achieve the above goals.

In the *cross-attention layer*, the uniform application of global text prompts across all frame tokens leads to severe semantic misalignment, which reduces the precision of multi-grained text-to-region control. To address this, we modulate cross-attention to amplify each local prompt’s focus on its corresponding spatial-disentangled region while suppressing attention to irrelevant areas. In the *self-attention layer*, pixels from one region may attend to outside or similar regions within the same class, leading to feature coupling and texture mixing, which is an inherent limitation of diffusion models that complicates multi-grained video editing. To mitigate this, we modulate self-attention to enhance feature separation by increasing intra-region focus and reducing inter-region interactions, ensuring each query attends only to its target region.

Our key contributions can be summarized as follows:

- To the best of our knowledge, this is the first attempt at multi-grained video editing. Our method enables both class-level, instance-level and part-level editing.
- We propose a novel framework, dubbed *ST-Modulator*, which modulates spatial-temporal cross- and self-attention for text-to-region control and feature separation between regions.
- Without tuning any parameters, we achieve state-of-the-art results on existing benchmarks and real-world videos both qualitatively and quantitatively.

2 RELATED WORK

2.1 TEXT-TO-IMAGE EDITING/GENERATION

In the realm of single attribute text-to-image editing, various approaches have been explored, from manipulating attention maps in Pix2Pix-Zero (Parmar et al., 2023) and Prompt2Prompt (Hertz et al., 2022) to employing masks in DiffEdit (Couairon et al., 2023) and Latent Blend (Avrahami et al., 2022; 2023) for foreground modifications while preserving the background.

For multi-grained editing, efforts like Attention and Excite (Chefer et al., 2023) and DPL (Wang et al., 2023b) focus on maximizing attention scores for each subject token and reducing attention leakage. In image generation, (Kim et al., 2023) modulates attention based on layout masks and dense captions, while (Phung et al., 2023) proposed an attention refocus loss for regularization. However, using single-frame layout masks and dense captioning alone is insufficient for video editing, as it fails to maintain the original video’s integrity and temporal consistency.

2.2 TEXT-TO-VIDEO EDITING

Video Editing based on Image Diffusion Models. Tune-A-Video (TAV) (Wu et al., 2022) is the first work to extend latent diffusion models to the spatial-temporal domain and encode the source motion implicitly by one-shot tuning but still fails to preserve local details. Fatezero (Qi et al., 2023) and Pix2Video (Ceylan et al., 2023) fuse self- or cross-attention maps in the inversion process for temporal consistency. However, (Qi et al., 2023) requires extensive RAM usage and suffers from layout preservation even when equipping TAV for local object editing. (Chai et al., 2023) and (Ouyang et al., 2023), following the Neural Atlas (Kasten et al., 2021) or dynamic Nerf’s deformation field (Mildenhall et al., 2021; Pumarola et al., 2021), struggle with non-grid human motion. Subsequent methods like Rerender-A-Video (Yang et al., 2023), Flatten (Cong et al., 2023) ControlVideo (Zhao et al., 2023a; Zhang et al., 2023b) achieve strict temporal consistency via optical-flow, depth/edge maps, but failed in multi-grained editing while preserving original layouts. Tokenflow (Geyer et al., 2023) enforces a linear mix of nearest key-frame features to ensure consistency but results in detail loss. Ground-A-VIDEO (Jeong & Ye, 2023) leverages groundings for multi-grained editing, but it suffers from feature mixing when bounding boxes overlap.

Video Editing based on Video Diffusion Models. Previous video editing work primarily utilized text-to-image SD model (Rombach et al., 2022). Recent advancements in video foundation models (Blattmann et al., 2023; Yu et al., 2023; Guo et al., 2023; Wang et al., 2023a) have led efforts like MotionDirector (Zhao et al., 2023b) and VideoSwap (Gu et al., 2023) to employ temporal priors for customized motion transfer. Yet, current video foundation models are limited to fixed views and struggle with non-grid human motions. Additionally, these editing methods require tuning parameters, which poses a challenge for real-time video editing applications. In contrast, our ST-Modulator method requires no parameter tuning, enabling zero-shot, multi-grained video editing.

3 METHOD

3.1 MOTIVATION

To investigate why previous methods failed in instance-level video editing (see Fig. 2), we begin with a basic analysis of the self-attention and cross-attention features within the diffusion model.

As shown in Fig. 3 (b), we apply K-Means clustering to the per-frame self-attention features during DDIM Inversion. Although the clustering captures a clear semantic layout, it fails to distinguish between distinct instances (e.g., “left man” and “right man”). Increasing the number of clusters leads to finer segmentation at the part level but does not resolve this issue, indicating that feature homogeneity across instances limits the diffusion model’s effectiveness in multi-grained video editing.

Next, we attempt to edit the same class of two men into different instances using SDEdit (Meng et al., 2021). However, Fig. 3 (d) shows that the weights for “Iron Man” and “Spiderman” overlap on the left man, and “blossoms” weight leaks onto the right man, resulting in the failed edit in (c).

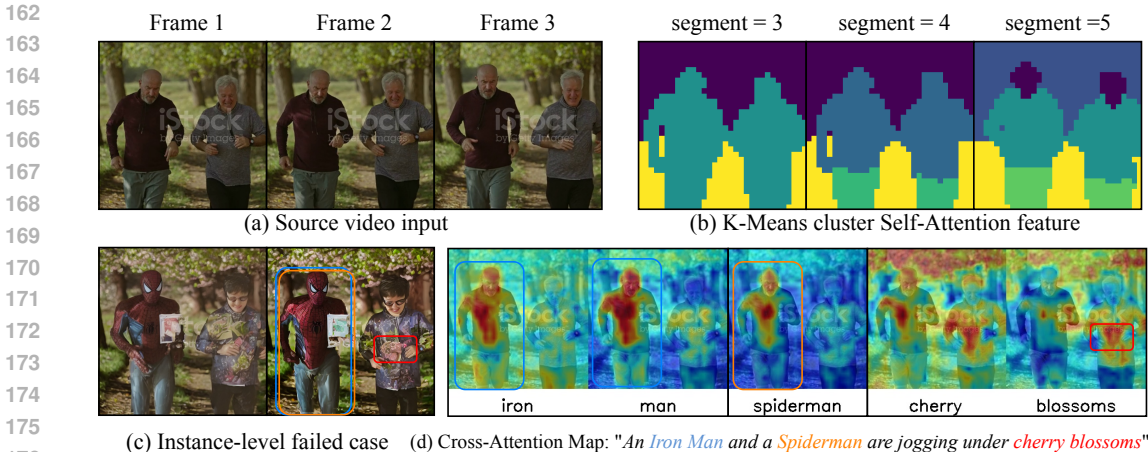


Figure 3: Analysis of why the diffusion model failed in instance-level video editing. Our goal is to edit left man into “Iron Man,” right man into “Spiderman,” and trees into “cherry blossoms.” In (b), we apply K-Means on self-attention, and in (d), we visualize the 32x32 cross-attention map.

Thus, for effective multi-grained editing, we pose the following question: *Can we modulate attention to ensure that each local edit’s attention weights are accurately distributed in the intended regions?*

To answer this, we propose ST-Modulator with two key designs: (1) Modulate cross-attention to induce textual features to congregate in corresponding spatial-disentangled regions, thereby enabling text-to-region control. (2) Modulate self-attention across the spatial-temporal axis to enhance intra-region focus and reduce inter-region interference, avoiding feature coupling within diffusion model.

3.2 PROBLEM FORMULATION

The purpose of this work is to perform multi-grained video editing across multiple regions based on the given prompts. This involves three hierarchical levels:

- (1) **Class-level editing:** Editing objects within the same class. (e.g., changing two men to “Spiderman,” where both belong to the human class, as seen in Fig. 2 second column)
- (2) **Instance-level editing:** Editing each individual instance to distinct object. (e.g., editing left man to “Spiderman,” right man to “Polar Bear,” as shown in Fig. 2 third column).
- (3) **Part-level editing:** Applying part-level edit to specific elements of individual instances. (e.g., adding “sunglasses ”when editing the right man to “Polar Bear” in Fig. 2 fourth column).

Given a source video $\mathbf{V} \in \mathbb{R}^{N \times 3 \times H \times W}$, where N is the number of frames, our goal is to obtain an edited video \mathbf{V}' based on specified edits. We aim to improve multi-grained control in video editing by conditioning on each region’s location and its text prompt. More formally, we optimize a video editing model $f(\tau_g, (\tau_1, m_1), \dots, (\tau_k, m_k))$, where τ_g is a global prompt, and (τ_k, m_k) are the k_{th} region’s prompt and corresponding location.

3.3 OVERALL FRAMEWORK

The proposed zero-shot multi-grained video editing pipeline is illustrated in Fig. 4 top. Initially, to retain high fidelity, we perform DDIM Inversion (Song et al., 2021) over the clean latent x_0 to get the noisy latent x_t . After the inversion process, we cluster the self-attention features to get the semantic layout as in Fig. 3 (b). Since self-attention features alone cannot distinguish between individual instances, we further employ SAM-Track (Cheng et al., 2023) to segment each instance. Finally, in the denoising process, we introduce ST-Layout Attn to modulate cross- and self-attention for text-to-region control and keep feature separation between regions, as detailed in Sec. 3.4.

Different from one global text prompt control of all frames, ST-Modulator allows paired instance- or part-level prompts and their locations to be specified in the denoising process. Our method is also versatile to ControlNet condition e , which can be depth or pose maps to provide structure condition.

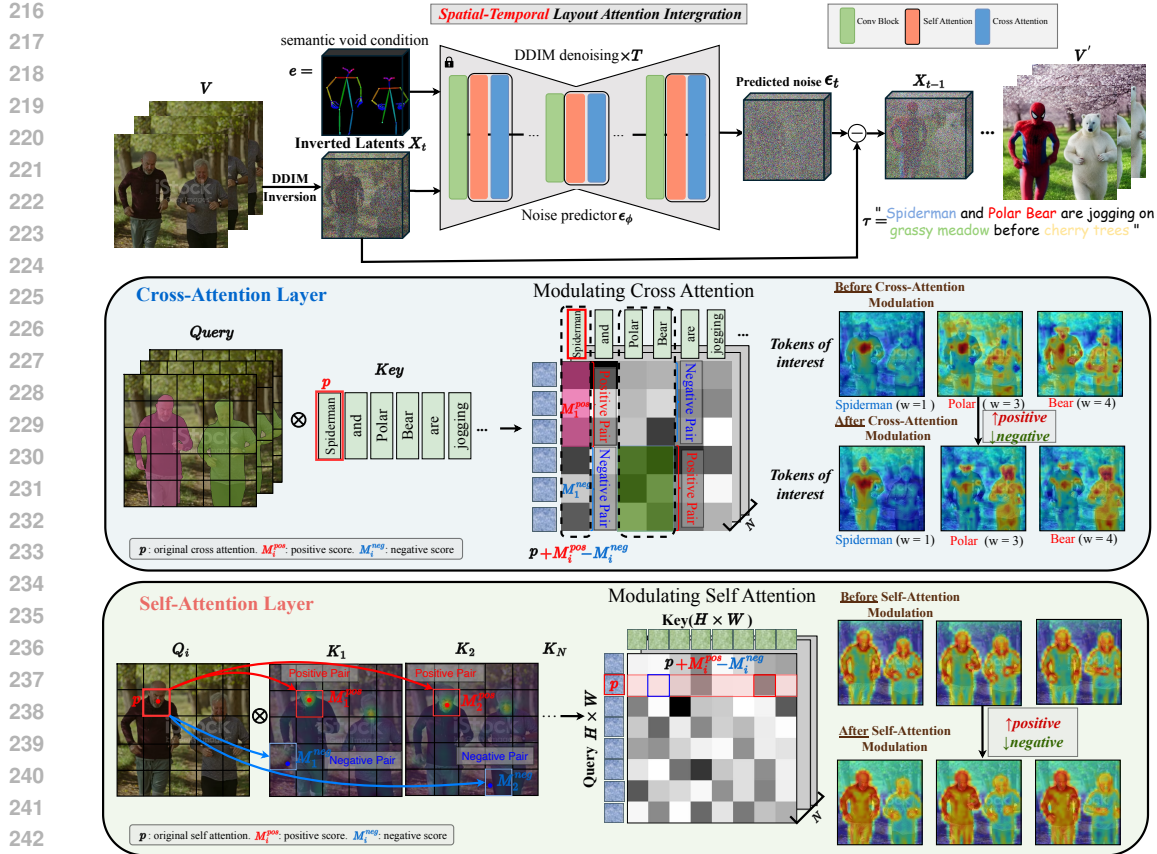


Figure 4: ST-Modulator pipeline. (1) we integrate ST-Layout Attn into the frozen SD for multi-grained editing, where we modulate self- and cross-attention in a unified manner. (2) In cross-attention, we view each local prompt and its location as positive pairs, while the prompt and outside-location areas are negative pairs, enabling text-to-region control. (3) In self-attention, we enhance positive awareness within intra-regions and restrict negative interactions between inter-regions across frames, making each query only attend to the target region and keep feature separation. In the bottom two figures, p denotes original attention score and w, i denotes the word and frame index.

3.4 SPATIAL-TEMPORAL LAYOUT-GUIDED ATTENTION

Based on the observation in Sec.3.1, cross-attention weight distribution adheres to the edit result. Meanwhile, self-attention is also crucial to generate temporal consistent video. However, the pixels in one region may attend to outside or similar regions, which poses an obstacle for multi-grained video editing. Therefore, we need to modulate both self- and cross-attention to make each pixel or local prompt only focus on the correct region.

To achieve this goal, we modulate both cross- and self-attention mechanisms via a unified increase positive and decrease negative manner. Specifically, for the i_{th} frame of the query feature, we modulate the query-key QK^T condition map as follows:

$$A_i^{\text{self/cross}} = \text{softmax}\left(\frac{QK^T + \lambda M^{\text{self/cross}}}{\sqrt{d}}\right), \quad (1)$$

$$M^{\text{self/cross}} = R_i \odot M_i^{\text{pos}} - (1 - R_i) \odot M_i^{\text{neg}},$$

where $R_i \in \mathbb{R}^{|\text{queries}| \times |\text{keys}|}$ indicates the query-key pair condition map at frame i , manipulating whether to increase or decrease the attention score for a particular pair. And $\lambda = \xi(t) \cdot (1 - S_i)$ is a regularization term. We follow the conclusion from (Kim et al., 2023), the $\xi(t)$ controls the modulation intensity across time-steps, allowing for gradual refinement of shape and appearance details. The latter is a size regulation term, making smaller region m_k subjected to larger modulation, enabling dynamic attention weight adjustments to layout size variations.

Modulate Cross-Attention for Text-to-Region Control. In the cross-attention layer, the textual feature serves as key and value, and interacts with the query feature from the video latent. Since each instance’s appearance and location are closely related to the cross-attention weight distribution, we aim to encourage each instance’s textual features to congregate in the corresponding location.

As shown in Fig. 4 mid, given the layout condition (τ_k, m_k) . For example, for $\tau_1 = \text{Spiderman}$, within the query-key cross-attention map, we can manually specify that the portion of the query feature corresponding to m_1 is positive, while all the remaining parts are designated as negative. Therefore, for each frame i , we can set the modulation value in cross attention layer as:

$$\begin{aligned} M_i^{\text{pos}} &= \max(QK^\top) - QK^\top, \\ M_i^{\text{neg}} &= QK^\top - \min(QK^\top), \end{aligned} \quad (2)$$

$$R_i^{\text{cross}}[x, y] = \begin{cases} m_{i,k}, & \text{if } y \in \tau_k \\ 0, & \text{otherwise} \end{cases}, \quad (3)$$

where x and y are the query and key indices, and R_i^{cross} is the query-key condition map in the cross attention layer. We regularize this condition map by initially broadcasting each region’s mask $m_{i,k}$ to its corresponding text key embedding K_{τ_k} , resulting in a condition map $R_i^{\text{cross}} \in \mathbb{R}^{(H \times W) \times L}$. Each sub-region intensity then adjusts gradually in the generation process. We set $M_i^{\text{pos/neg}}$ based on the gap between max/min values and the original scores, to keep modulated values within the original range. Our modulation is applied to all frames to achieve spatial-temporal region control.

As shown in Fig. 4 (mid right), after adding positive and subtracting negative values, the original cross-attn weight of “Spiderman” (e.g., p) is amplified and focused on the left man. While the distract weight of “polar” “bear” become concentrated on the right man. These indicate our modulation redistributes each prompt’s weight align with target areas, enabling precise text-to-region control.

Modulate Self-Attention to Keep Feature Separation. To adapt the T2I model for T2V editing, we treat the full video as “a larger picture,” replacing spatial attention with spatial-temporal self-attention while retaining the pretrained weights. This enhances cross-frame interaction and provides a broader visual context. However, naive self-attention can cause regions to attend to irrelevant or similar areas (e.g., Fig. 4 bottom, before modulation query p attend to two-man), which leads to mixed texture. To address this, we need to strengthen positive focus within the same region and restrict negative interactions between different regions.

As shown in Fig. 4 (bottom left), the maximum cross-frame diffusion feature indicates the strongest response among tokens within the same region. Note that DIFT (Tang et al., 2023) uses this to match different images, while we focus on cross-frame correspondences and intra-region attention modulation in the generation process. Nevertheless, negative inter-region correspondence is equally crucial for decoupling feature mixing. Beyond DIFT, we find that the minimum cross-frame diffusion feature similarity effectively captures the relations between tokens across different regions. Therefore, we define the spatial-temporal positive/negative values as:

$$\begin{aligned} M_i^{\text{pos}} &= \max(Q_i[K_1, \dots, K_n]^\top) - Q_i[K_1, \dots, K_n]^\top, \\ M_i^{\text{neg}} &= Q_i[K_1, \dots, K_n]^\top - \min(Q_i[K_1, \dots, K_n]^\top). \end{aligned} \quad (4)$$

To ensure each patch attends to intra-regions feature while avoiding interaction in inter-regions feature. We define the spatial-temporal query-key condition map:

$$R_i^{\text{self}}[x, y] = \begin{cases} 0, \forall j \in [1 : N], \text{ if } m_{i,k}[x] \neq m_{j,k}[y] \\ 1, \text{ otherwise} \end{cases}. \quad (5)$$

For frame indices i and j , the value is zero when tokens belong to different instances across frames.

As shown in the right part of Fig. 4 bottom, after applying our self-attention modulation, the query feature from the left man’s nose (e.g., p) attends only to the left instance, avoiding distraction to the right instance. This demonstrates that our self-attention modulation breaks the diffusion model’s class-level feature correspondence, ensuring feature separation at the instance level.

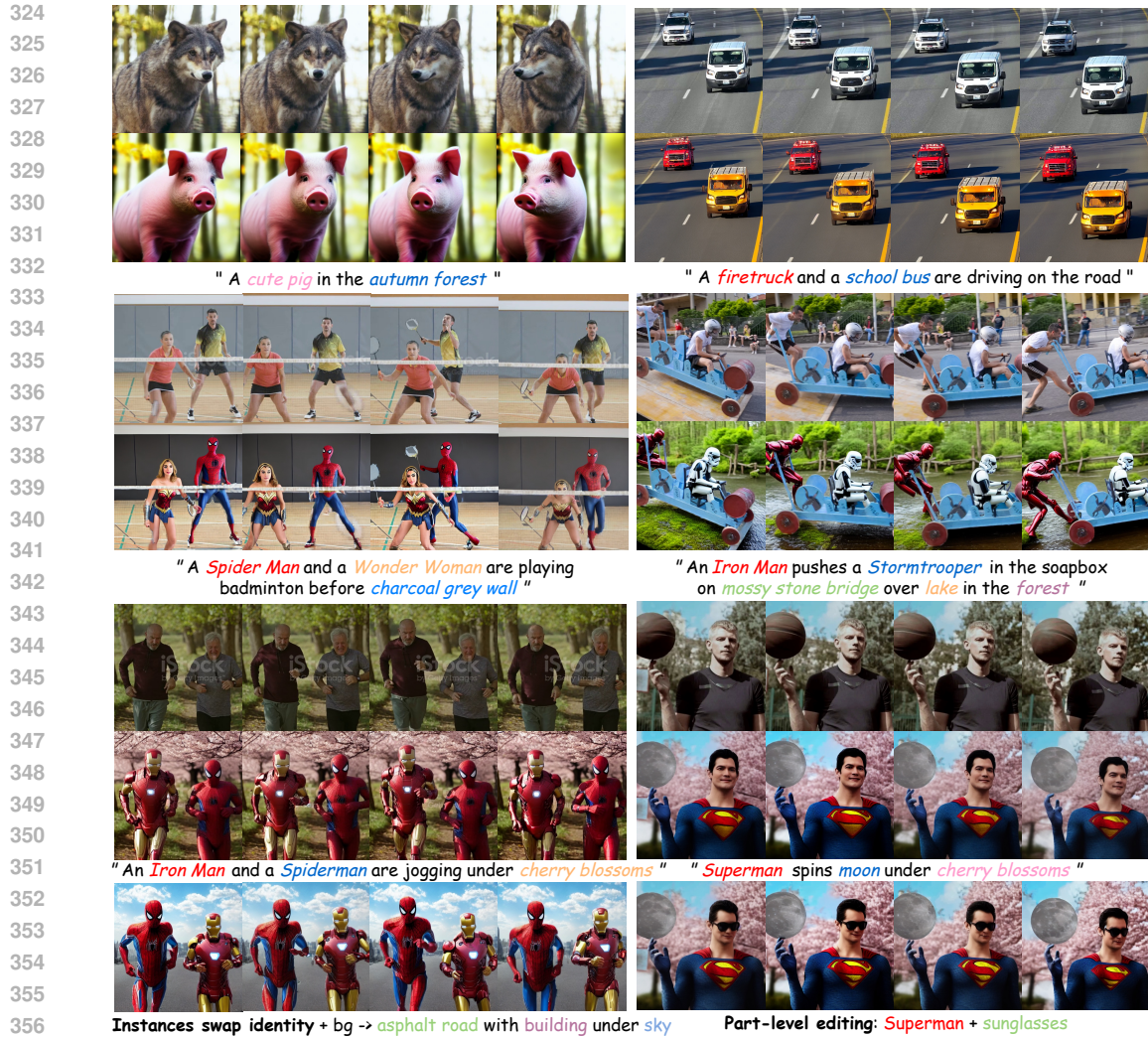


Figure 5: Qualitative results of ST-Modulator. Our method is versatile for general objects like animals, cars, and humans while also supporting instance identity swapping and part-level editing.

4 EXPERIMENTS

4.1 EXPERIMENTAL SETTINGS

In the experiment, we adopt the pretrained Stable Diffusion v1.5 as the base model, using 50 steps of DDIM inversion and denoising. Our ST-Modulator operates in a zero-shot manner, requiring no additional parameter tuning. To enhance memory efficiency, we re-engineer slice attention within our ST Layout Attn. ST Layout Attn is applied during the first 15 denoising steps. We set $\xi(t) = 0.3 \cdot t^5$ for self-attention and $\xi(t) = t^5$ for cross-attention, where the timestep $t \in [0, 1]$ is normalized. All The experiments are conducted on an NVIDIA A40 GPU. We evaluate our ST-Modulator using a dataset of 76 video-text pairs, including videos from DAVIS (Perazzi et al., 2016), TGVE¹, and the Internet², with 16-32 frames per video. Four automatic metrics are employed for evaluation: CLIP-T, CLIP-F, Warp-Err, and Q-edit, following (Wu et al., 2022; Cong et al., 2023). All metrics are scaled by 100 for clarity. For baselines, we compare against T2I-based methods, including FateZero (Qi et al., 2023), ControlVideo (Zhang et al., 2023b), TokenFlow (Geyer et al., 2023), GroundVideo (Jeong & Ye, 2023) and T2V-based DMT (Yatim et al., 2024). For all of these baseline methods, we follow the default settings from their official GitHub repositories. For fairness, all T2I baselines are equipped with same ControlNet conditions.

¹<https://sites.google.com/view/loveucvpr23/track4>

²<https://www.istockphoto.com/> and <https://www.pexels.com/>

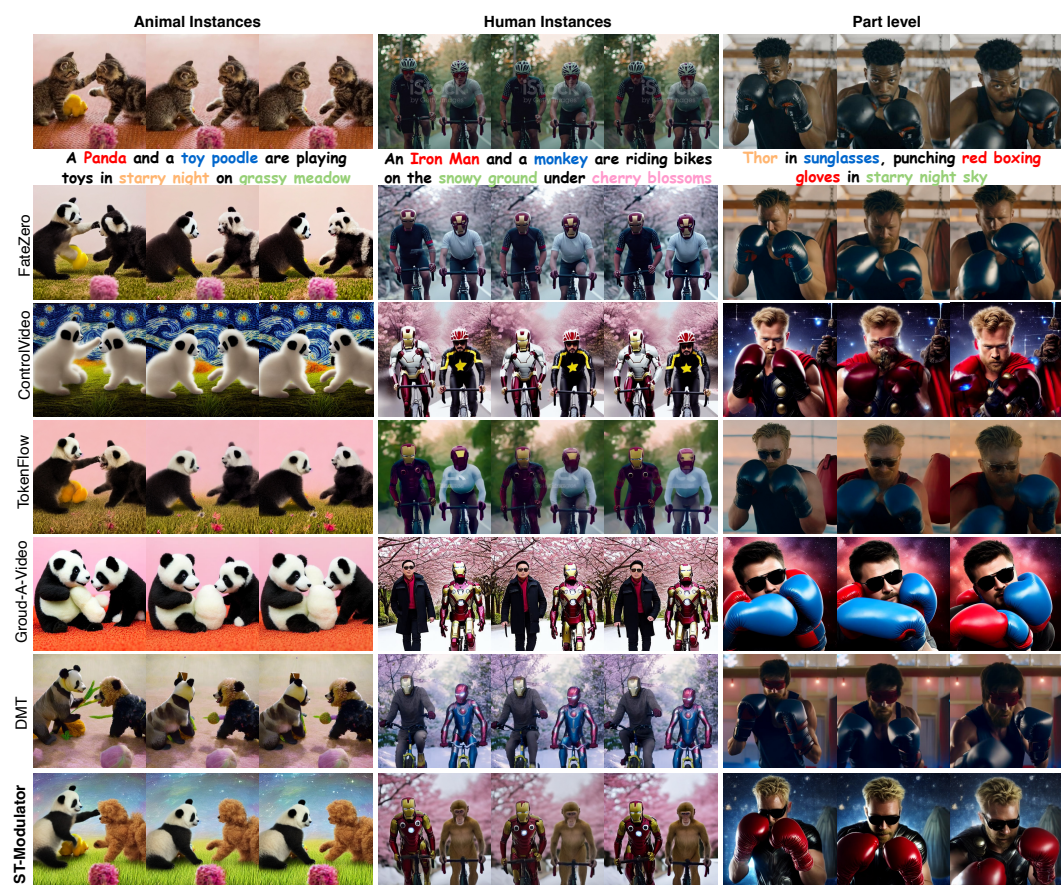


Figure 6: Qualitative comparisons. We refer the reader to our [project page](#) for detailed assessment.

4.2 RESULTS

We evaluate ST-Modulator on videos covering class-level, instance-level, and part-level edits. Our method demonstrates versatility in handling animals, such as transforming a “wolf” into a “pig” (Fig. 5, top left). For instance-level editing, we can modify vehicles separately (e.g., transforming an “SUV” into a “firetruck” and a “van” into a “school bus”) in Fig. 5, top right. ST-Modulator excels at editing multiple instances in complex, occluded scenes, like “Spider-Man and Wonder Woman playing badminton” (Fig. 5, middle left). Previous methods often struggle with such non-rigid motion. In addition, our method is capable of multi-region editing, where both foreground and background are edited, as shown in the soap-box scene, where the background changes to “a mossy stone bridge over a lake in the forest” (Fig. 5, middle right). Thanks to precise attention weight distribution, we can swap identities seamlessly, such as in the jogging scene, where “Iron Man” and “Spider-Man” swap identities (Fig. 5, bottom left). For part-level edits, ST-Modulator excels in adjusting a character to wear a Superman suit while keeping sunglasses intact (Fig. 5, bottom right). Overall, for multi-grained editing, our ST-Modulator demonstrates outstanding performance.

4.3 QUALITATIVE AND QUANTITATIVE COMPARISONS

Qualitative Comparison. Figure 6 shows a comparison between ST-Modulator and baseline methods, including T2I-based and T2V-based approaches, for instance-level and part-level editing. For fairness, all T2I-based methods use ControlNet conditioning. **(1) Animal instances:** In the left column, T2I-based methods like FateZero, ControlVideo, and TokenFlow edit both cats into pandas due to same-class feature coupling in diffusion models, failing to perform separate edits. DMT, even with video generation priors, still blends the panda and toy poodle features. In contrast, ST-Modulator successfully edits one into a panda and the other into a toy poodle. **(2) Human instances:** In the middle column, baselines struggle with same-class feature coupling, partially editing both men into

Method	Automatic Metric				Human Evaluation		
	CLIP-F \uparrow	CLIP-T \uparrow	Warp-Err \downarrow	Q-edit \uparrow	Edit-Acc \uparrow	Temp-Con \uparrow	Overall \uparrow
FateZero	95.75	33.78	3.08	10.96	59.8	78.6	59.6
ControlVideo	97.71	34.41	4.73	7.27	53.2	50.0	43.6
TokenFlow	96.48	34.59	2.82	12.28	45.4	50.4	39.8
Ground-A-Video	95.17	35.09	4.43	7.92	69.0	72.0	63.2
DMT	96.34	34.09	2.05	16.63	58.7	79.4	64.5
ST-Modulator(ours)	98.63	36.56	1.42	25.75	88.4	85.0	83.0

Table 1: Quantitative comparison of automatic metrics and human evaluation. The best results are **bolded**.

Iron Man. DMT and Ground-A-Video also fail to follow user intent, incorrectly editing the left and right instances. ST-Modulator, however, correctly transforms the right man into a monkey, breaking the human-class limitation. **(3) Part-level editing:** In the third column, ST-Modulator manages part-level edits, such as sunglasses and boxing gloves. ControlVideo edits the gloves but struggles with sunglasses and motion consistency. TokenFlow and DMT edit the sunglasses but fail to modify the gloves or background. In comparison, ST-Modulator achieves both instance-level and part-level edits, significantly outperforming previous methods.

Quantitative Comparison. We compare the performance of different methods using both automatic metrics and human evaluation. **CLIP-T** calculates the average cosine similarity between the input prompt and all video frames, while **CLIP-F** measures the average cosine similarity between consecutive frames. Additionally, **Warp-Err** captures pixel-level differences by warping the edited video frames according to the optical flow of the source video, extracted using RAFT-Large (Teed & Deng, 2020). To provide a more comprehensive measure of video editing quality, we follow (Cong et al., 2023) and use **Q-edit**, defined as CLIP-T/Warp-Err. For clarity, we scale all automatic metrics by 100. In terms of human evaluation, we assess three key aspects: **Edit-Accuracy** (whether each local edit is accurately applied), **Temporal Consistency** (evaluated by participants for coherence between video frames), and **Overall Edit Quality**. We invited 20 participants to rate 76 video-text pairs on a scale of 20 to 100 across these three criteria, following (Jeong & Ye, 2023). As demonstrated in Table 1, ST-Modulator consistently outperforms both T2I- and T2V-based methods. This is primarily due to ST-Layout Attn’s precise text-to-region control and maintaining feature separation between regions. As a result, our method achieves significantly higher CLIP-T and Edit-Accuracy scores compared to other baselines. The improved Warp-Err and Temporal Consistency metrics further indicate that ST-Modulator delivers temporally coherent video edits.

Efficiency Comparison. To evaluate efficiency, we compared baselines with ST-Modulator on a single A6000 GPU for editing 16 video frames. The metrics include editing time (time taken to perform one edit) and both GPU and CPU memory usage. From Tab. 2, it is clear our method achieves the fastest editing time with the lowest memory usage, indicating its computational efficiency.

	Time(min) \downarrow	Memory (GB) \downarrow	RAM (GB) \downarrow	W/O ST-Layout Attn	Attn Weight Before	Attn Weight After	ST-Layout Attn
FateZero	8.68	27.35	144.22				
ControlVideo	4.41	16.15	7.03				
TokenFlow	4.56	17.84	5.35				
Ground-A-Video	5.81	17.31	9.96				
DMT	5.79	27.88	8.12				
ST-Modulator	3.83	15.94	4.42				

Table 2: Efficiency comparison.

Figure 7: Attention weight distribution.

4.4 ABLATION STUDY

To assess the contributions of different components in our proposed ST-Layout Attn, we first evaluate whether our attention can achieve attention weight distribution, then decouple the self-attention modulation and cross-attention modulation to evaluate their individual effectiveness.

Attention Weight Distribution. We evaluate the impact of ST-Layout Attn on attention weight distribution. As shown in Fig. 7, the target prompt is “An Iron Man is playing tennis on a snow court.” We visualize the cross-attention map for “man” to assess weight distribution. Without ST-Layout Attn, feature mixing occurs, with “snow” weight spilling onto “Iron Man.” With ST-Layout Attn, the man’s weight is correctly distributed. This is because we enhance positive pair scores and suppress negative pairs in both cross- and self-attention. This enables precise, separate edits for “Iron Man” and “snow.” Additional visualizations are in the Appendix.

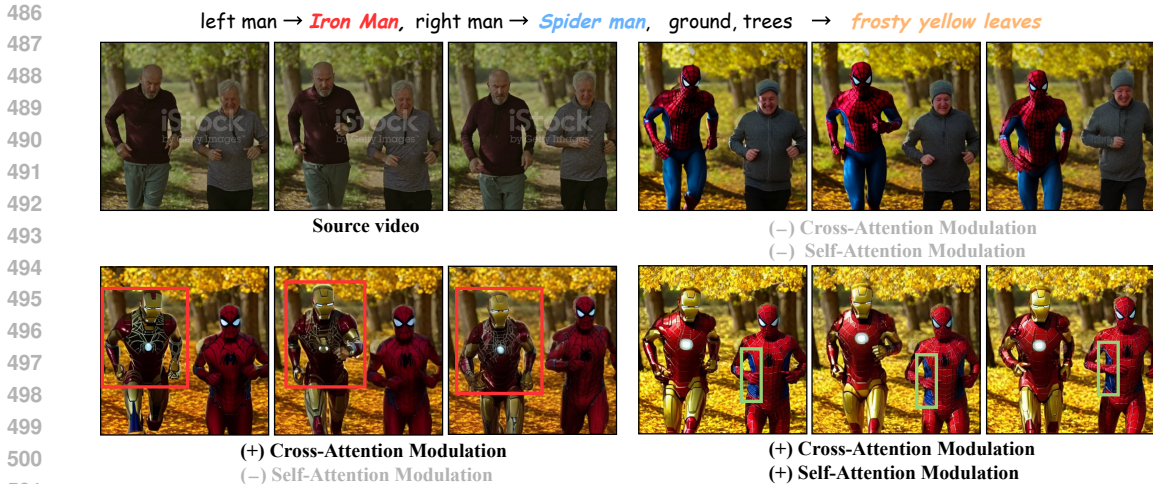


Figure 8: Ablation of cross- and self-modulation in ST-Layout Attn.

Method	CLIP-F ↑	CLIP-T ↑	Warp-Err ↓	Q _{edit} ↑
Baseline	95.21	33.59	3.86	8.70
Baseline + Cross Modulation	96.28	36.09	2.53	14.26
Baseline + Cross Modulation + Self Modulation	98.63	36.56	1.42	25.75

Table 3: Quantitative ablation of cross- and self-modulation in ST-Layout Attn.

511 **Cross-Attention Modulation.** In Fig. 8 and Tab. 3, we illustrate video editing results under different
 512 set up: (1) Baseline (2) Baseline + Cross-Attn Modulation (3) Baseline + Cross-Attn Modulation +
 513 Self-Attn Modulation. As shown in Fig. 8 top right, direct editing fails to discriminate between the
 514 left and right instances, leading to incorrect (left) or no edits(right). However, when equipped with
 515 cross-attention modulation, we achieve accurate text-to-region control, thereby editing left man to
 516 “Iron Man” and right man to “Spiderman” separately. The quantitative results in Tab. 3 indicate that
 517 with cross-attention modulation (second row), CLIP-T increases by 7.4%, and Q-edit increases by
 518 63.9%. This demonstrates the effectiveness of our cross-attention modulation.

519 **Self-Attention Modulation.** However, modulating only cross-attention still leads to structure dis-
 520 tortions, such as the *spider web* appearing on the left man. This is caused by the coupling of same
 521 class-level features (e.g., human). When using our self-attention modulation, the feature mixing is
 522 significantly reduced, and the left man retains unique object features. This is achieved by decreas-
 523 ing the negative pair scores between different instances, while increasing positive scores within the
 524 same instance. As a result, more part-level details, such as the distinctive *blue sides*, are generated
 525 in the optimized areas. The quantitative decrease in Warp-Err by 43.9% and increase in Q-edit by
 526 80.6% in Tab. 3 further prove the effectiveness of self-attention modulation.

527

528 **5 CONCLUSION**

529

530

531 In this paper, we aim to solve the problem of multi-grained video editing, which includes both
 532 class-level, instance-level and part-level video editing. To the best of our knowledge, this is the first
 533 attempt at this task. In this task, we find that the key problem is that the diffusion model views
 534 different instances as same-class features and direct global editing will mix different local regions.
 535 To wrestle with these problems, we propose ST-Modulator to modulate spatial-temporal cross- and
 536 self-attention for text-to-region control while keeping feature separation between regions. In cross-
 537 attention, we enhance each local prompt’s focus on its corresponding spatial-disentangled region
 538 while suppressing attention to irrelevant areas, thereby enabling text-to-region control. In self-
 539 attention, we increase intra-region awareness and reduce inter-region interactions to keep feature
 separation between regions. Extensive experiments demonstrate that our ST-Modulator surpasses
 previous video editing methods on both class-level, instance-level, and part-level video editing.

6 ETHICS STATEMENT

This project aims to solve multi-grained video editing. However, the potential misuse of this technology, such as the creation of deceptive videos by altering identities, poses a risk. Strategies like incorporating invisible watermarking could be explored to ensure videos are not used maliciously.

REFERENCES

<https://www.pika.art/>. URL <https://www.pika.art/>.

Omri Avrahami, Dani Lischinski, and Ohad Fried. Blended diffusion for text-driven editing of natural images. In *Proceedings of the IEEE/CVF Conference on Computer Vision and Pattern Recognition*, pp. 18208–18218, 2022.

Omri Avrahami, Ohad Fried, and Dani Lischinski. Blended latent diffusion. *ACM Transactions on Graphics (TOG)*, 42(4):1–11, 2023.

Andreas Blattmann, Robin Rombach, Huan Ling, Tim Dockhorn, Seung Wook Kim, Sanja Fidler, and Karsten Kreis. Align your latents: High-resolution video synthesis with latent diffusion models. In *Proceedings of the IEEE/CVF Conference on Computer Vision and Pattern Recognition*, pp. 22563–22575, 2023.

Tim Brooks, Bill Peebles, Connor Holmes, Will DePue, Yufei Guo, Li Jing, David Schnurr, Joe Taylor, Troy Luhman, Eric Luhman, Clarence Ng, Ricky Wang, and Aditya Ramesh. Video generation models as world simulators. 2024. URL <https://openai.com/research/video-generation-models-as-world-simulators>.

Duygu Ceylan, Chun-Hao P Huang, and Niloy J Mitra. Pix2video: Video editing using image diffusion. In *Proceedings of the IEEE/CVF International Conference on Computer Vision*, pp. 23206–23217, 2023.

Wenhao Chai, Xun Guo, Gaoang Wang, and Yan Lu. Stablevideo: Text-driven consistency-aware diffusion video editing. In *Proceedings of the IEEE/CVF International Conference on Computer Vision*, pp. 23040–23050, 2023.

Hila Chefer, Yuval Alaluf, Yael Vinker, Lior Wolf, and Daniel Cohen-Or. Attend-and-excite: Attention-based semantic guidance for text-to-image diffusion models. *ACM Transactions on Graphics (TOG)*, 42(4):1–10, 2023.

Haoxin Chen, Yong Zhang, Xiaodong Cun, Menghan Xia, Xintao Wang, Chao Weng, and Ying Shan. Videocrafter2: Overcoming data limitations for high-quality video diffusion models. In *Proceedings of the IEEE/CVF Conference on Computer Vision and Pattern Recognition*, pp. 7310–7320, 2024.

Yangming Cheng, Liulei Li, Yuanyou Xu, Xiaodi Li, Zongxin Yang, Wenguan Wang, and Yi Yang. Segment and track anything. *arXiv preprint arXiv:2305.06558*, 2023.

Yuren Cong, Mengmeng Xu, Christian Simon, Shoufa Chen, Jiawei Ren, Yanping Xie, Juan-Manuel Perez-Rua, Bodo Rosenhahn, Tao Xiang, and Sen He. Flatten: optical flow-guided attention for consistent text-to-video editing. *arXiv preprint arXiv:2310.05922*, 2023.

Guillaume Couairon, Jakob Verbeek, Holger Schwenk, and Matthieu Cord. Diffedit: Diffusion-based semantic image editing with mask guidance. In *ICLR 2023 (Eleventh International Conference on Learning Representations)*, 2023.

Michal Geyer, Omer Bar-Tal, Shai Bagon, and Tali Dekel. Tokenflow: Consistent diffusion features for consistent video editing. *arXiv preprint arXiv:2307.10373*, 2023.

Yuchao Gu, Yipin Zhou, Bichen Wu, Licheng Yu, Jia-Wei Liu, Rui Zhao, Jay Zhangjie Wu, David Junhao Zhang, Mike Zheng Shou, and Kevin Tang. Videoswap: Customized video subject swapping with interactive semantic point correspondence. *arXiv preprint arXiv:2312.02087*, 2023.

- 594 Yuwei Guo, Ceyuan Yang, Anyi Rao, Yaohui Wang, Yu Qiao, Dahua Lin, and Bo Dai. Animatediff:
595 Animate your personalized text-to-image diffusion models without specific tuning. *arXiv preprint*
596 *arXiv:2307.04725*, 2023.
- 597 Amir Hertz, Ron Mokady, Jay Tenenbaum, Kfir Aberman, Yael Pritch, and Daniel Cohen-Or.
598 Prompt-to-prompt image editing with cross attention control. 2022.
- 600 Hyeonho Jeong and Jong Chul Ye. Ground-a-video: Zero-shot grounded video editing using text-
601 to-image diffusion models. *arXiv preprint arXiv:2310.01107*, 2023.
- 602 Yoni Kasten, Dolev Ofri, Oliver Wang, and Tali Dekel. Layered neural atlases for consistent video
603 editing. *ACM Transactions on Graphics (TOG)*, 40(6):1–12, 2021.
- 604 Yunji Kim, Jiyoung Lee, Jin-Hwa Kim, Jung-Woo Ha, and Jun-Yan Zhu. Dense text-to-image
605 generation with attention modulation. In *ICCV*, 2023.
- 606 Yuheng Li, Haotian Liu, Qingyang Wu, Fangzhou Mu, Jianwei Yang, Jianfeng Gao, Chunyuan Li,
607 and Yong Jae Lee. Gligen: Open-set grounded text-to-image generation. *CVPR*, 2023.
- 608 Shaoteng Liu, Yuechen Zhang, Wenbo Li, Zhe Lin, and Jiaya Jia. Video-p2p: Video editing with
609 cross-attention control. In *Proceedings of the IEEE/CVF Conference on Computer Vision and*
610 *Pattern Recognition*, pp. 8599–8608, 2024.
- 611 Chenlin Meng, Yutong He, Yang Song, Jiaming Song, Jiajun Wu, Jun-Yan Zhu, and Stefano Ermon.
612 SDEdit: Guided image synthesis and editing with stochastic differential equations. 2021.
- 613 Ben Mildenhall, Pratul P Srinivasan, Matthew Tancik, Jonathan T Barron, Ravi Ramamoorthi, and
614 Ren Ng. Nerf: Representing scenes as neural radiance fields for view synthesis. *Communications*
615 *of the ACM*, 65(1):99–106, 2021.
- 616 Hao Ouyang, Qiuyu Wang, Yuxi Xiao, Qingyan Bai, Juntao Zhang, Kecheng Zheng, Xiaowei Zhou,
617 Qifeng Chen, and Yujun Shen. Codef: Content deformation fields for temporally consistent video
618 processing. *arXiv preprint arXiv:2308.07926*, 2023.
- 619 Gaurav Parmar, Krishna Kumar Singh, Richard Zhang, Yijun Li, Jingwan Lu, and Jun-Yan Zhu.
620 Zero-shot image-to-image translation. In *ACM SIGGRAPH 2023 Conference Proceedings*, pp.
621 1–11, 2023.
- 622 Federico Perazzi, Jordi Pont-Tuset, Brian McWilliams, Luc Van Gool, Markus Gross, and Alexander
623 Sorkine-Hornung. A benchmark dataset and evaluation methodology for video object segmen-
624 tation. In *Proceedings of the IEEE conference on computer vision and pattern recognition*, pp.
625 724–732, 2016.
- 626 Quynh Phung, Songwei Ge, and Jia-Bin Huang. Grounded text-to-image synthesis with attention
627 refocusing. *arXiv preprint arXiv:2306.05427*, 2023.
- 628 Albert Pumarola, Enric Corona, Gerard Pons-Moll, and Francesc Moreno-Noguer. D-nerf: Neural
629 radiance fields for dynamic scenes. In *Proceedings of the IEEE/CVF Conference on Computer*
630 *Vision and Pattern Recognition*, pp. 10318–10327, 2021.
- 631 Chenyang Qi, Xiaodong Cun, Yong Zhang, Chenyang Lei, Xintao Wang, Ying Shan, and Qifeng
632 Chen. Fatezero: Fusing attentions for zero-shot text-based video editing. *arXiv preprint*
633 *arXiv:2303.09535*, 2023.
- 634 Robin Rombach, Andreas Blattmann, Dominik Lorenz, Patrick Esser, and Björn Ommer. High-
635 resolution image synthesis with latent diffusion models. In *Proceedings of the IEEE/CVF confer-*
636 *ence on computer vision and pattern recognition*, pp. 10684–10695, 2022.
- 637 Jiaming Song, Chenlin Meng, and Stefano Ermon. Denoising diffusion implicit models. In *Interna-*
638 *tional Conference on Learning Representations*, 2021.
- 639 Luming Tang, Menglin Jia, Qianqian Wang, Cheng Perng Phoo, and Bharath Hariharan. Emer-
640 gent correspondence from image diffusion. In *Thirty-seventh Conference on Neural Information*
641 *Processing Systems*, 2023. URL <https://openreview.net/forum?id=yPOiXjdfnU>.

- 648 Zachary Teed and Jia Deng. Raft: Recurrent all-pairs field transforms for optical flow. In *Computer*
649 *Vision—ECCV 2020: 16th European Conference, Glasgow, UK, August 23–28, 2020, Proceedings,*
650 *Part II 16*, pp. 402–419. Springer, 2020.
- 651
- 652 Jiuniu Wang, Hangjie Yuan, Dayou Chen, Yingya Zhang, Xiang Wang, and Shiwei Zhang. Mod-
653 elscope text-to-video technical report. *arXiv preprint arXiv:2308.06571*, 2023a.
- 654 Kai Wang, Fei Yang, Shiqi Yang, Muhammad Atif Butt, and Joost van de Weijer. Dynamic
655 prompt learning: Addressing cross-attention leakage for text-based image editing. *arXiv preprint*
656 *arXiv:2309.15664*, 2023b.
- 657
- 658 Jay Zhangjie Wu, Yixiao Ge, Xintao Wang, Weixian Lei, Yuchao Gu, Wynne Hsu, Ying Shan,
659 Xiaohu Qie, and Mike Zheng Shou. Tune-a-video: One-shot tuning of image diffusion models
660 for text-to-video generation. *arXiv preprint arXiv:2212.11565*, 2022.
- 661 Shuai Yang, Yifan Zhou, Ziwei Liu, , and Chen Change Loy. Rerender a video: Zero-shot text-
662 guided video-to-video translation. In *ACM SIGGRAPH Asia Conference Proceedings*, 2023.
- 663
- 664 Danah Yatim, Rafail Fridman, Omer Bar-Tal, Yoni Kasten, and Tali Dekel. Space-time diffusion
665 features for zero-shot text-driven motion transfer. In *Proceedings of the IEEE/CVF Conference*
666 *on Computer Vision and Pattern Recognition*, pp. 8466–8476, 2024.
- 667 Lijun Yu, Yong Cheng, Kihyuk Sohn, José Lezama, Han Zhang, Huiwen Chang, Alexander G
668 Hauptmann, Ming-Hsuan Yang, Yuan Hao, Irfan Essa, et al. Magvit: Masked generative video
669 transformer. In *Proceedings of the IEEE/CVF Conference on Computer Vision and Pattern Recog-*
670 *nition*, pp. 10459–10469, 2023.
- 671 Lvmin Zhang, Anyi Rao, and Maneesh Agrawala. Adding conditional control to text-to-image
672 diffusion models. In *Proceedings of the IEEE/CVF International Conference on Computer Vision*
673 *(ICCV)*, pp. 3836–3847, October 2023a.
- 674
- 675 Yabo Zhang, Yuxiang Wei, Dongsheng Jiang, Xiaopeng Zhang, Wangmeng Zuo, and Qi Tian. Con-
676 trolvideo: Training-free controllable text-to-video generation. *arXiv preprint arXiv:2305.13077*,
677 2023b.
- 678 Min Zhao, Rongzhen Wang, Fan Bao, Chongxuan Li, and Jun Zhu. Controlvideo: Adding condi-
679 tional control for one shot text-to-video editing. *arXiv preprint arXiv:2305.17098*, 2023a.
- 680
- 681 Rui Zhao, Yuchao Gu, Jay Zhangjie Wu, David Junhao Zhang, Jiawei Liu, Weijia Wu, Jussi Keppo,
682 and Mike Zheng Shou. Motiondirector: Motion customization of text-to-video diffusion models.
683 *arXiv preprint arXiv:2310.08465*, 2023b.
- 684
- 685
- 686
- 687
- 688
- 689
- 690
- 691
- 692
- 693
- 694
- 695
- 696
- 697
- 698
- 699
- 700
- 701

A EVALUATE SAM-TRACK MASKS' IMPACT

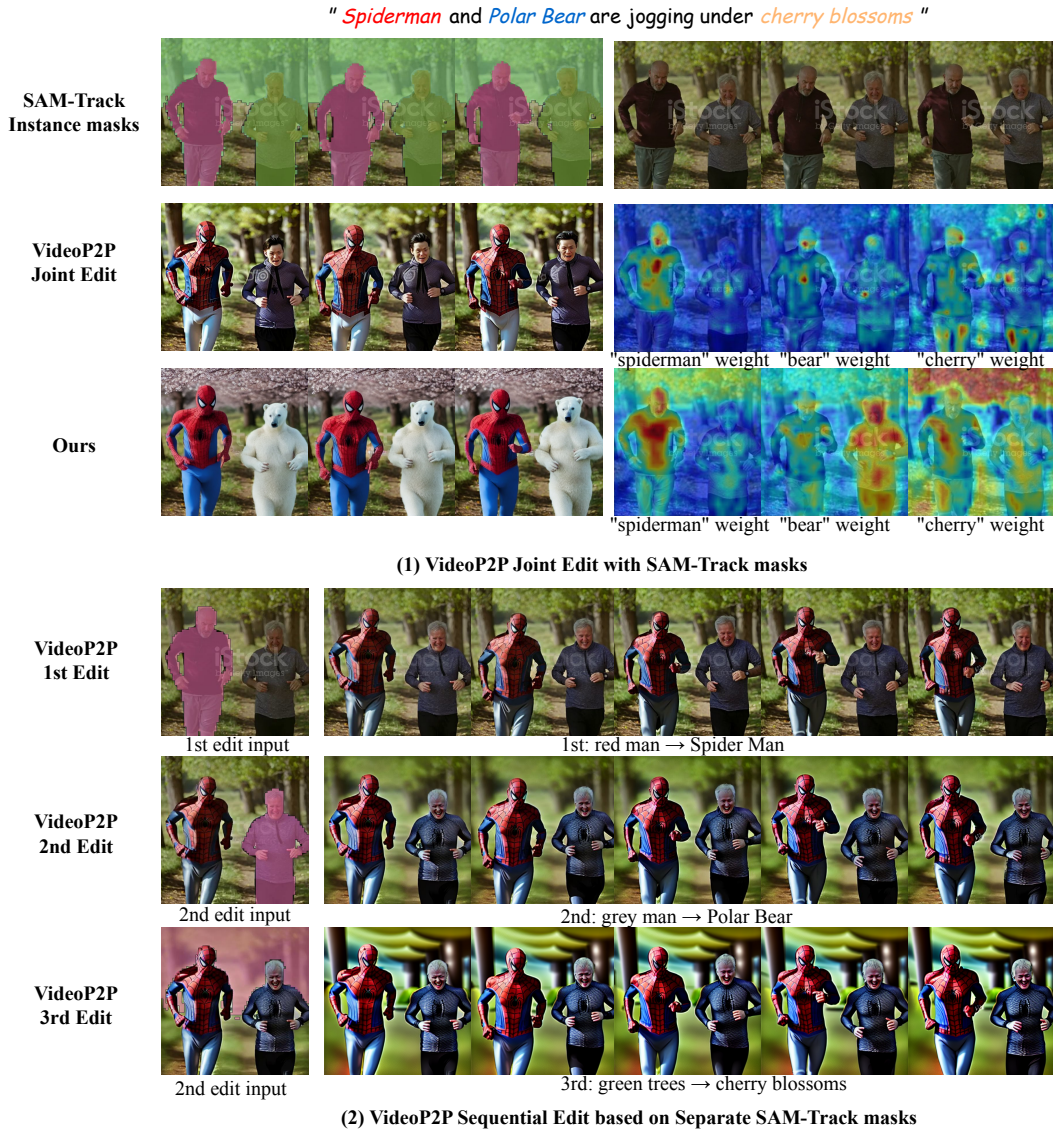
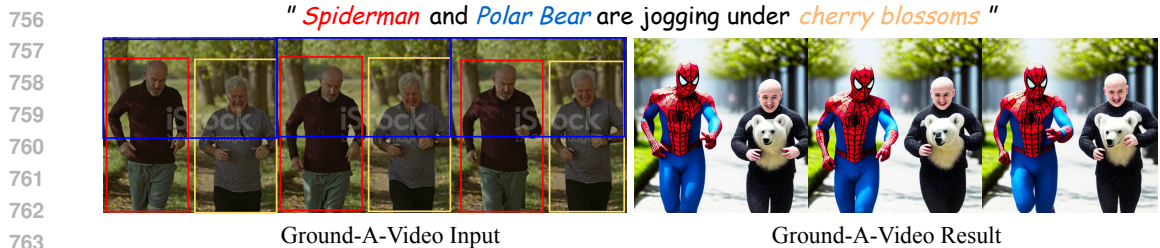


Figure 9: VideoP2P joint and sequential edit with SAM-Track masks

To evaluate the impact of using SAM-Track (Cheng et al., 2023) for instance segmentation, we compare our ST-Modulator against VideoP2P (Liu et al., 2024), which is equipped with SAM-Track instance masks. The instance masks replace cross-attention masks during editing. A 16-frame one-shot tuning is performed, and ControlNet conditioning Zhang et al. (2023a) is added for fairness. Two experiments are tested: (1) jointly editing multiple areas in a single denoising process and (2) sequentially editing three areas by inputting separate masks.

Results show that joint editing (Fig. 9(1)) modifies only left man into "Spiderman," leaving other areas unchanged due to inaccurate cross-attn weight distribution. Sequential editing (Fig. 9(2)) succeeds initially but fails later due to error accumulation in denoising, resulting in blurred details.



765 **Figure 10:** Ground-A-Video joint edit with instance information

766

767

768 Additionally, as shown in figure above 10, also in Figs 2 and 6, Ground-A-Video (Jeong & Ye, 2023)

769 struggles with multi-grained video editing tasks, even with instance-level grounding information

770 (e.g., text-to-bounding box), which is comparable to SAM-Track’s masks.

771 These comparisons indicate that while SAM-Track provides layout guidance, it does not guarantee

772 successful edits. In contrast, our method enables zero-shot multi-instance editing, which was not

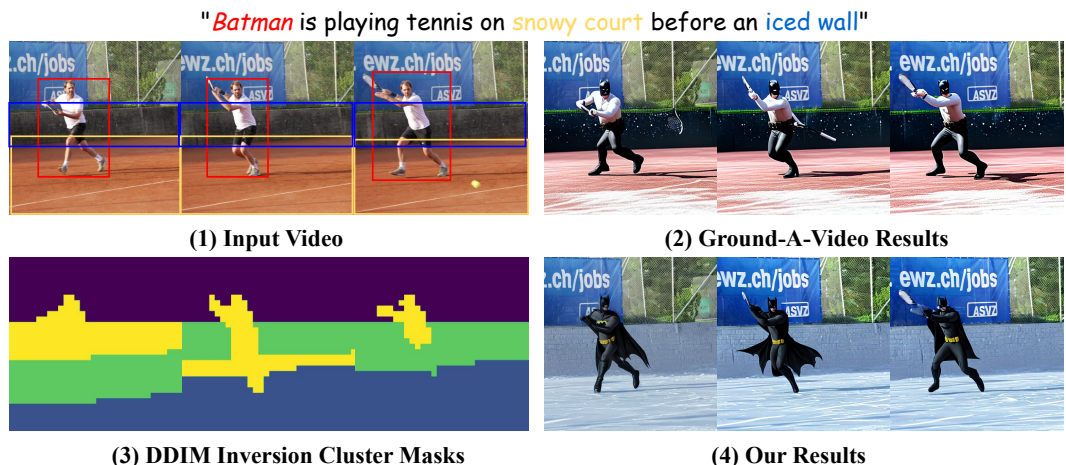
773 achievable by any previous methods, even when providing existing SOTA with SAM-Track masks.

774

775

776 **B ST-MODULATOR CAN WORK WITHOUT SAM-TRACK MASKS**

777



794 **Figure 11:** Our method without additional SAM-Track masks

795

796

797 Our method is not strictly dependent on SAM-Track masks. As shown in Fig.11(3), we can cluster

798 DDIM inversion self-attention features to get unaccurate coarse layouts. Our method still achieves

799 high-quality multi-area editing results (4). In contrast, even with precise groundings (converted from

800 SAM-Track masks in (1)), Ground-A-Video fails to edit all three regions. These comparisons indi-

801 cates that our method does not rely on SAM-Track segmentation. Instead, it works effectively only

802 using the self-attention feature inside the diffusion model, even without accurate layout guidance.

803

804

805 **C SOLELY EDIT ON SPECIFIC SUBJECTS, BACKGROUND UNCHANGED**

806

807

808 Our method is designed for multi-area editing and can naturally perform background-preserved

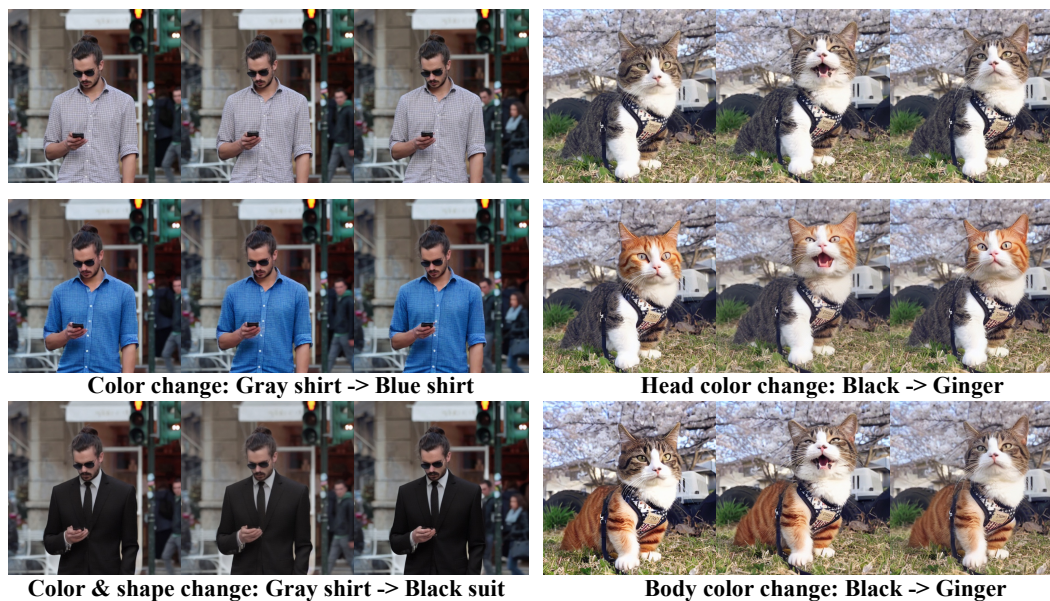
809 subject editing, as it treats multi-area editing as selecting regions restricted to the foreground. As

shown in Fig 12, our method can separately edit the “left man” and “right man” or jointly edit both

subjects while keeping the background unchanged.



823 **Figure 12: Soely edit on specific subjects, background unchanged**



844 **Figure 13: Part-level modifications on humans and animals**

847 D PART-LEVEL MODIFICATION EXAMPLES

849 Our part-level editing supports not only adding objects but also part-level attribute modifications. In the human case (Fig. 13 left), our method change the color of a gray shirt to blue (second row) and edit a half-sleeve shirt into a black suit (third row), showcasing part-level attribute and structure editing. Similarly, in the animal case, our method can changes a cat’s head or body color from black to ginger while preserving the belt’s color, demonstrating precise part-level modifications.

857 E TEMPORAL FOCUS OF ST-LAYOUT ATTN

859 Our ST-Layout Attn is designed as a full-frame approach to ensure inter-frame consistency. As shown in Fig. 14, per-frame ST-Layout Attn causes feature coupling on Iron Man, while the sparse-causal method results in flickering and misses Spider Man’s blue details due to their limited receptive fields for positive/negative value selection across different layouts. In contrast, our ST-Layout Attn effectively preserves texture details and prevents flickering, achieving temporal consistent and layout unified multi-grained video editing.

864
865
866
867
868
869
870
871
872
873
874
875
876
877
878
879
880
881
882
883
884
885
886
887
888
889
890
891
892
893
894
895
896
897
898
899
900
901
902
903
904
905
906
907
908
909
910
911
912
913
914
915
916
917

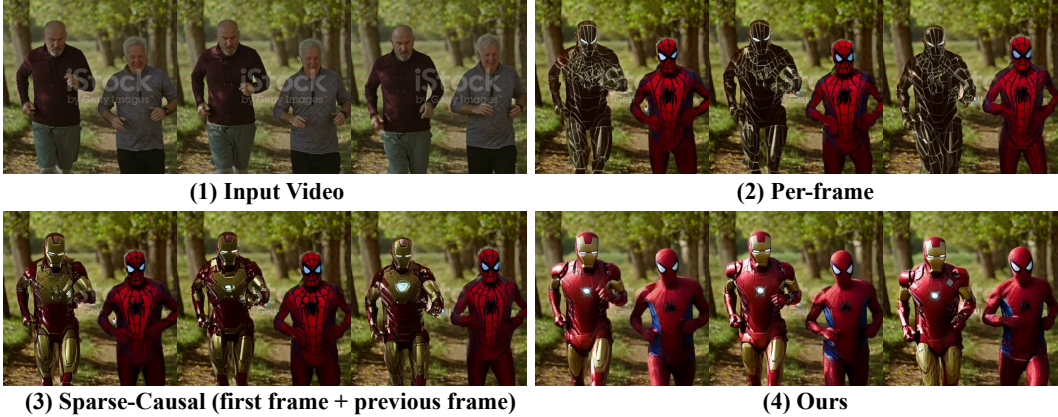


Figure 14: Temporal Focus of ST-Layout Attn

F CONTROLNET ABLATION



Figure 15: ControlNet ablation

Our method utilizes ControlNet depth/pose conditioning in certain complex motion cases to provide necessary structural guidance. As shown in Fig. 15, even without ControlNet, our method can still achieve simultaneous multi-region editing. However, in such cases, there may be some structural inconsistencies between the edit object and source object due to the lack of explicit structure guidance.

G MORE GENERAL OBJECTS AND SHAPE EDITING

H MORE VISUALIZATION

I LATENT BLEND

To preserve areas not intended for editing (i.e., τ_3 in $\Delta_\tau = \{\tau_1 \rightarrow \tau_{1'}, \tau_2 \rightarrow \tau_{2'}, \tau_3 \rightarrow \tau_3, \dots\}$), we employ Latent Blend (Avrahami et al., 2022; 2023), which leverages masks to direct the model focus on areas requiring editing while keeping the background region identical to the source video.

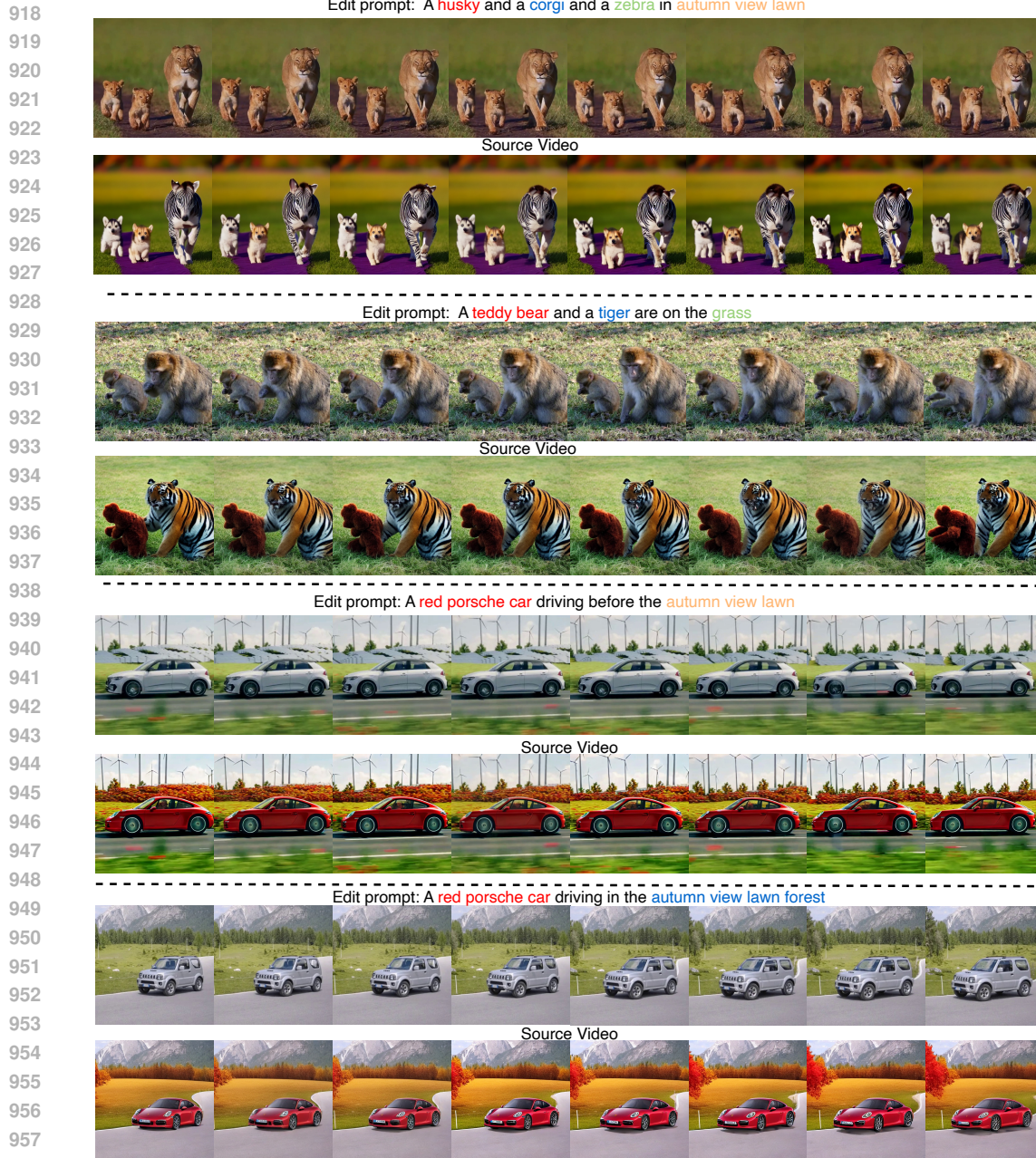
For each frame i in the video, we first merge each attribute mask to form the global foreground mask M_i by applying the logical OR operation across all layouts masks $m_{i,k} = [m_{i,1}, m_{i,2}, \dots, m_{i,k}]$:

$$M_i = m_{i,1} \vee m_{i,2} \vee \dots \vee m_{i,k}. \tag{6}$$

We aggregate the masks M_i from all frames to obtain a combined mask M , and then blend the latent states z_t at each timestep t during the denoising process as follows:

$$z_t = (1 - M) \cdot \tilde{z}_t + M \cdot z_t, \tag{7}$$

where \tilde{z}_t indicates the latent feature in the DDIM inversion process and z_t is corresponding latent feature during the DDIM denoising process.



959 **Figure 16:** More general objects instance editing (animals) and shape editing (cars) results.

960

961

962 The key behind employing Latent Blend for preserving the background is that, given a desired area

963 mask, the less noisy foreground latent can be guided by the target text prompt Δ_T . Meanwhile, the

964 latent features outside the mask (the background) can be preserved. This blending ensures that, even

965 if the latent feature within the edit area is modified, the background features stay consistent.

967 J EXPERIMENTAL DETAILS

968

969 For FateZero³ (Qi et al., 2023), we employ prompt-to-prompt (Hertz et al., 2022) replace editing. To

970 enhance the identity binding of the edited object, we set the self/cross replacement steps at 0.3 and

971 ³<https://github.com/ChenyangQiQi/FateZero>

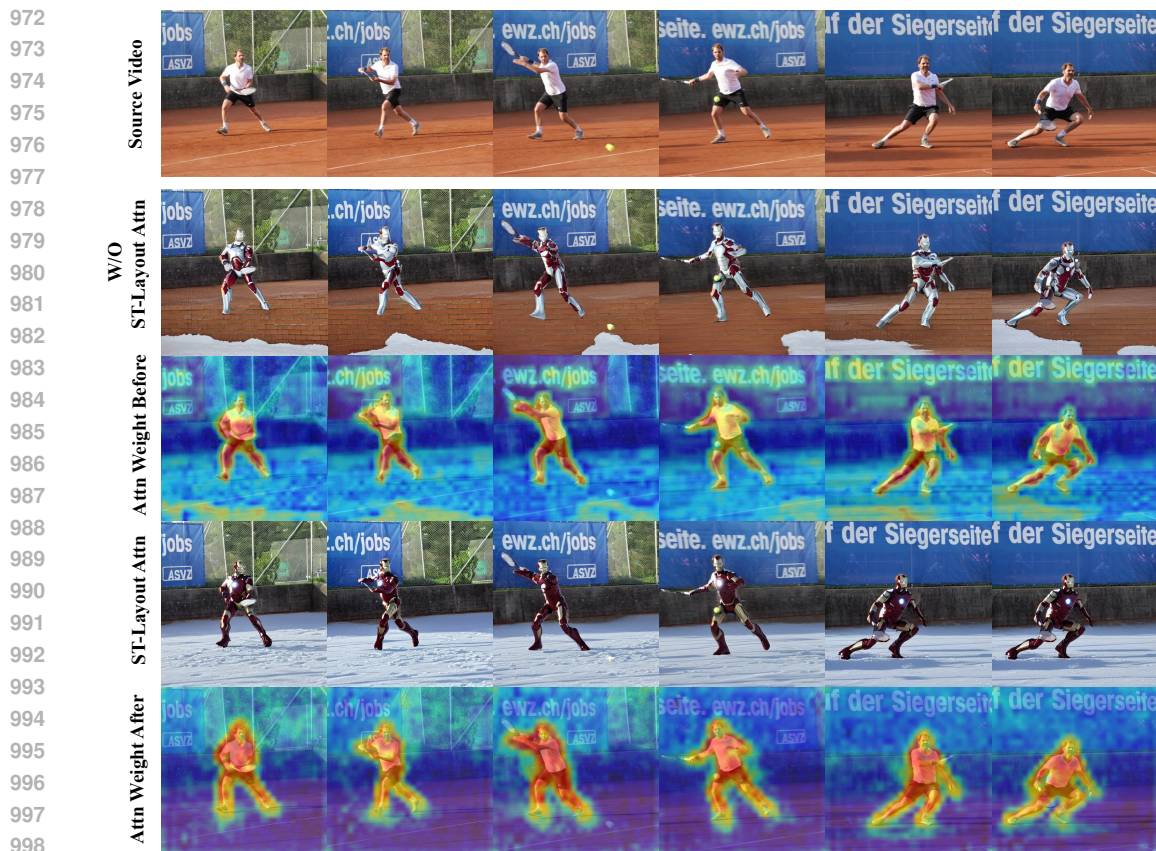


Figure 17: More frames ablation of ST-Layout Attn’s effects on attention weight distribution.

the blending threshold at 0.7. In TokenFlow⁴ (Geyer et al., 2023), we utilize SD editing and default to 4 keyframes for 16-frame videos. For other comparative methods like ControlVideo⁵ (Zhang et al., 2023b) and GroundVideo⁶ (Jeong & Ye, 2023) and DMT⁷ (Yatim et al., 2024), we adhere to their default hyperparameter settings. To ensure fairness across all T2I-based methods compared, we re-implement ControlNet (Zhang et al., 2023a) on their codebases.

K LIMITATIONS.

First, although our method can achieve multi-grained editing of video, the generation quality is still limited by the base model since we are a training-free method. In scenarios where the generation prior to SD is not ideal, artifacts may occur in the editing results. Second, since our method is based on a T2I model, it struggles with large shape deformations and significant appearance changes. This limitation is inherent in zero-shot methods. A potential future direction is to incorporate motion priors from T2V generation models (Chen et al., 2024; Wang et al., 2023a) to handle such challenges.

⁴<https://github.com/omerbt/TokenFlow>

⁵<https://github.com/YBYB2hang/ControlVideo>

⁶<https://github.com/Ground-A-Video/Ground-A-Video>

⁷<https://github.com/diffusion-motion-transfer/diffusion-motion-transfer>